The Astrophysical Journal, 585:1024–1037, 2003 March 10

ECCENTRICITY EVOLUTION FOR PLANETS IN GASEOUS DISKS

Peter Goldreich and Re'em Sari
Mail Code 130-33, California Institute of Technology, Pasadena, CA 91125
Received 2002 February 25; accepted 2002 November 19

ABSTRACT

At least several percent of solar-type stars possess giant planets. Surprisingly, most move on orbits of substantial eccentricity. We investigate the hypothesis that interactions between a giant planet and the disk from which it forms promote eccentricity growth. These interactions are concentrated at discrete Lindblad and corotation resonances. Interactions at principal Lindblad resonances cause the planet's orbit to migrate and open a gap in the disk if the planet is sufficiently massive. Those at first-order Lindblad and corotation resonances change the planet's orbital eccentricity. Eccentricity is excited by interactions at external Lindblad resonances that are located on the opposite side of corotation from the planet, and damped by co-orbital Lindblad resonances that overlap the planet's orbit. If the planet clears a gap in the disk, the rate of eccentricity damping by co-orbital Lindblad resonances is reduced. Density gradients associated with the gap activate eccentricity damping by corotation resonances at a rate that initially marginally exceeds that of eccentricity excitation by external Lindblad resonances. But the corotation torque may be reduced as the result of the trapping of fluid in libration around potential maxima. This nonlinear saturation can tip the balance in favor of eccentricity excitation. A minimal initial eccentricity of the order of 1% is required to overcome viscous diffusion, which acts to unsaturate corotation resonances by reestablishing the large-scale density gradient. Thus, eccentricity growth is a finite-amplitude instability. Formally, the apsidal resonance, which is a special kind of co-orbital Lindblad resonance that exists in pressure-dominated disks, appears to damp eccentricity faster than external Lindblad resonances can excite it. However, the wavelength of the apsidal wave in a pressure-dominated disk is so long that it does not propagate. A self-gravity–dominated disk does not have an apsidal resonance. Nevertheless, apsidal waves are excited at gap edges. Although these propagate, their long wavelengths suggest that they are likely to be reflected at disk edges to form standing waves. Viscous damping of standing waves results in eccentricity damping, but at level far below that which traveling waves would produce. Although the level of eccentricity damping due to apsidal waves is reduced to a modest level in both pressure- and self-gravity–dominated disks, whether it drops well below that of Lindblad resonances depends sensitively on the disk's thickness and planet's mass. However, our analysis shows that with reasonable parameters, planet-disk interactions can promote eccentricity growth.

Subject headings: planetary systems: formation — planetary systems: protoplanetary disks

1. INTRODUCTION

As of today, there are 100 extrasolar planets listed on the California and Carnegie Planet Search Web page.[1] Almost all of the 78 planets with periods greater than 20 days move on orbits of substantial eccentricity, both the mean and median being 0.33. By contrast, the 14 planets with periods less than 7 days have low-eccentricity orbits, 0.02 mean and 0.01 median, apparently the result of eccentricity damping associated with tides raised in the planets by their central stars. The critical period separating small- from large-eccentricity orbits implies that extrasolar planets have tidal quality factors $Q \sim 10^5$, similar to that of Jupiter.

Solar system planets, with the exception of Mercury, have low-eccentricity orbits.[2] Thus, the large orbital eccentricities of extrasolar planets came as a surprise. How might they have arisen? Interactions among planets have been the focus of most previous suggestions (Rasio & Ford 1996; Lin & Ida 1997; Weidenschilling & Marzari 1996; Ford, Havlickova, & Rasio 2001; Chiang, Fischer, & Thommes 2002). In systems with isolated planets, these involve speculative scenarios in which planets either were ejected from the system (Rasio & Ford 1996) or merged with the remaining planet (Lin & Ida 1997). Less attention has been paid to interactions between planets and the disks from which they formed. Analytic theory is not capable of resolving whether these interactions can produce eccentricity growth. However, it can identify crucial issues and thus provide guidance for targeted simulations. That is the goal of our paper.

Our investigation applies results derived in studies of satellite interactions with planetary rings by Goldreich & Tremaine (1979, 1980) and later extended by Ward (1986) and Artymowicz (1993a, 1993b). Goldreich & Tremaine (1980, 1981) conclude that interactions at Lindblad resonances excite orbital eccentricity of both narrow rings and their shepherd satellites, whereas those at corotation resonances damp it. However, the balance between excitation and damping is a precarious one; damping exceeds driving by about 4.6% provided that the corotation resonances are unsaturated. Ward (1986) and Artymowicz (1993a) point out that interactions at co-orbital Lindblad resonances damp its orbital eccentricity. The latter estimates that, in a gapless disk, damping by co-orbital Lindblad resonances is about a factor of 3 more rapid than excitation by external Lindblad resonances. In recent papers, Ward & Hahn (1998, 2000) claim that interactions at apsidal resonances, which damp eccentricity, are more potent than those at

[1] California and Carnegie Planet Search home page is available at: http://exoplanets.org/almanac.html.

[2] We consider Pluto to be a member of the Kuiper belt and not a bona fide planet.

ordinary Lindblad resonances. On balance, current opinion favors the notion that planet-disk interactions damp eccentricity. We suggest that for massive planets the opposite may be true.

The structure of our paper is as follows. In § 2, we argue following Rasio & Ford (1996) and Ford et al. (2001) that planet-planet interactions cannot account for the prevalence of eccentric orbits among isolated planets. Section 3 reviews the effects on eccentricity of planet-disk interactions at Lindblad, corotation, and apsidal resonances. We demonstrate in § 4 that interactions at apsidal resonances are much less effective at damping eccentricity than previous estimates suggest. Section 5 is devoted to an evaluation of the balance between eccentricity damping at Lindblad resonances which overlap the planet's orbit and eccentricity excitation at those which lie either inside or outside it. A planet that clears a sufficiently clean gap tilts the balance in favor of net eccentricity excitation by Lindblad resonances. However, linear theory predicts that corotation resonances enforce eccentricity damping. This leads to § 6, in which we argue that torques at corotation resonances are weakened by saturation, provided that the planet's orbital eccentricity is at least 1%.

In assembling the case that orbital eccentricities of extrasolar planets may result from planet-disk interactions, we discuss three new results.

1. A correction to the standard Lindblad torque formula for apsidal resonances which applies when apsidal waves either do not propagate or are trapped by reflecting at disk boundaries.
2. An account of the balance between eccentricity excitation by Lindblad resonances and eccentricity damping by corotation resonances in a gap where the pressure gradient reduces the epicyclic frequency of the gas to a value that is much smaller than its orbital frequency.
3. Physical descriptions of the nonlinear saturation of corotation torques in both particle (Goldreich & Tremaine 1981) and gas (Ogilvie & Lubow 2002) disks, including an explanation for their similarities.

2. PLANET-PLANET INTERACTIONS

Is the observed eccentricity distribution of extrasolar planets the result of planet-planet interactions? In particular, can they account for the following properties?

1. Typical eccentricities are of the order of a few tenths.
2. Eccentricities smaller than one-tenth are rare except for planets with orbital periods less than 20 days, for which tidal friction is likely to have damped eccentricity.
3. Most of the planets discovered to date are not currently involved in a significant interaction with another planet of comparable or larger mass.

For planet-planet interactions to produce an eccentric orbit for an isolated planet requires at least one planet to disappear. The missing planet might have collided and merged with the remaining planet or effectively merged as a result of tidal capture. It might also have been ejected from the system or fallen into the central star. Numerical integrations of systems with two equal-mass planets on initially circular orbits by Ford et al. (2001) produce a much greater fraction of isolated planets with low-eccentricity orbits than is observed. These are a consequence of mergers which Ford et al. (2001) assume to occur whenever the separation between the planets drops below the sum of their radii. But the case against planet-planet interactions is even stronger than the results of Ford et al. (2001) indicate, because they neglect tidal captures. Taking the tidal capture cross section for $n = 1$ polytropes from Kim & Lee (1999), and the relative velocity at infinity as numerically calculated by Rasio & Ford (1996), we estimate a critical impact parameter for tidal capture between 2 and 3 times larger than the two radii assumed for merger by Rasio & Ford (1996) and Ford et al. (2001).

Next, we consider some aspects of the merger process for a system whose initial state consists of two planets, each having mass M_p and radius R_p, moving on coplaner circular orbits with radii r_1 and r_2 around a star of mass M_* and radius R_*. We assume that the final state consists of a single or binary planet with mass $2M_p$ moving on an orbit with semimajor axis a and eccentricity e.[3] Applying conservation of energy and angular momentum, we relate the final orbit to the initial ones by

$$E = -\frac{GM_*M_p}{a} = -\frac{GM_*M_p}{2r_1} - \frac{GM_*M_p}{2r_2} - \Delta E \quad (1)$$

and

$$\begin{aligned} H &= 2M_p\sqrt{GM_*a(1-e^2)} \\ &= M_p\left(\sqrt{GM_*r_1} + \sqrt{GM_*r_2}\right) - \Delta H\ . \end{aligned} \quad (2)$$

Here ΔE and ΔH are the energy and angular momentum stored internally in either the merger product or the relative orbit of the binary. Energy dissipated by impact or through tidal dissipation is accounted for by an increase of the binding energy.

We estimate ΔE and ΔH by noting that when the planets are separated by less than the Hill radius, $r_{\rm Hill} \equiv (M_p/3M_*)^{1/3}a$, they are effectively a two-body system. Thus,[4]

$$\frac{\Delta E}{E} \lesssim \frac{M_p a}{M_* r_{\rm Hill}} \sim \left(\frac{M_p}{M_*}\right)^{2/3}\ . \quad (3)$$

Moreover, since merging or tidal capture requires that the planet-planet periapse distance be no larger than a few times R_p,

$$\left|\frac{\Delta H}{H}\right| \sim \left(\frac{M_pR_p}{M_*a}\right)^{1/2} \sim \left(\frac{M_p}{M_*}\right)^{2/3}\left(\frac{R_*}{a}\right)^{1/2}\ . \quad (4)$$

The final expressions for $\Delta E/E$ and $\Delta H/H$ follow from the assumption that the planet and star have similar densities. In what follows we discard $|\Delta H/H| \ll \Delta E/E$, since $R_*/a \ll 1$.

Eccentricity is related to orbital energy and angular momentum by

$$e^2 = 1 + \frac{2H^2E}{(2M_p)^3(GM_*)^2}\ . \quad (5)$$

[3] Orbital elements for a binary refer to its center of mass.

[4] Ford et al. (2001) provide a derivation similar to ours. However, they incorrectly assume that $\Delta E/E \lesssim (M_p/M_*)^{1/2}$, which leads to a higher eccentricity estimate.

Substituting for E and H using equations (1) and (2) yields

$$e^2 = \frac{1}{4}\left(3 - \frac{r_1^2 + r_2^2}{2r_1 r_2} - \sqrt{\frac{r_1}{r_2}} - \sqrt{\frac{r_2}{r_1}}\right) - \frac{(r_1 + r_2 + 2\sqrt{r_1 r_2})\Delta E}{4GM_* M_p} . \tag{6}$$

Taking the leading contribution in $|r_1 - r_2|/(r_1 + r_2)$ and writing

$$\frac{\Delta E}{E} = -A\left(\frac{M_p}{M_*}\right)^{2/3} , \tag{7}$$

where $A \lesssim 1$, we deduce that the eccentricity is bounded by

$$e^2 = A\left(\frac{M_p}{M_*}\right)^{2/3} - \frac{3}{4}\left(\frac{r_1 - r_2}{r_1 + r_2}\right)^2 . \tag{8}$$

Maximal eccentricity is achieved if the initial orbits have the same semimajor axis. Mergers or captures are not possible for initial separations much larger than the Hill radius. We conclude that merging and tidal capture cannot produce eccentricities of more than a few percent for Jupiter-like planets.

Our discussion of planet-planet interactions giving rise to orbital eccentricities is far from exhaustive. Here we briefly mention a scenario analyzed by Chiang et al. (2002). In it, two planets undergo differential orbital migration which causes the ratio of their mean motions to diverge. Passage through mean motion resonances is shown to lead to eccentricity growth. A shortcoming of this work is that although planet-disk interactions are taken to be responsible for orbital migration, their direct effects on eccentricity evolution are not accounted for.

3. PLANET-DISK INTERACTION: GENERAL

The gravitational potential of a planet can be expanded in a Fourier series in azimuthal angle θ and time t. Each term of this series is proportional to $\cos[m(\theta - \Omega_{l,m}t)]$ and has a radius-dependent amplitude $\phi_{l,m}(r)$. The mean motion Ω_p is the unique pattern speed for a planet with a circular orbit. From here on, subscripts p and d denote planet and disk, respectively. Pattern speeds for a planet that moves on an eccentric orbit may contain harmonics of the epicyclic frequency κ_p and are denoted by $\Omega_{l,m} = \Omega_p + (l - m)\kappa_p/m$. To first order in eccentricity e_p, each value of m contributes three components: a principal one with pattern speed $\Omega_{m,m} = \Omega_p$ whose amplitude $\phi_{m,m}$ is independent of e_p, and two first-order components with pattern speeds[5] $\Omega_{m\pm1,m} = \Omega_p \pm \kappa_p/m$ whose amplitudes $\phi_{m\pm1,m}$ are proportional to e_p.[6]

Two kinds of resonance are associated with each potential component. Corotation resonances occur where the pattern speed matches the angular velocity of the disk material, $\Omega_{l,m} = \Omega_d$. A disk particle located at a corotation resonance experiences a constant torque, which causes the radius of its orbit to change but does not excite its epicyclic motion. Lindblad resonances occur where the disk's angular velocity differs from the pattern speed such that $m(\Omega_d - \Omega_{l,m}) = \pm\kappa_d$. The two Lindblad resonances associated with each potential component are distinguished by the adjectives "inner" and "outer" and are often denoted as ILR and OLR. A disk particle located at a Lindblad resonance is subject to radial and azimuthal perturbation forces which vary at its epicyclic frequency. These excite its epicyclic motion and also change its semimajor axis.

Each m has nine resonances associated with it: three potential components $\phi_{m,m}$ and $\phi_{m\pm1,m}$, and three resonances for each potential component. Table 1 describes some properties of these resonances.

3.1. *Understanding the Sign of the Torque*

Each potential component is constant in a frame rotating with its pattern speed $\Omega_{l,m}$, so its perturbations of the disk's angular momentum H_d and energy E_d must preserve the Jacobi constant $J_{l,m} = E_d - \Omega_{l,m}H_d$. Thus,

$$\frac{dE_d}{dt} = \Omega_{l,m}\frac{dH_d}{dt} = \Omega_{l,m}T_d , \tag{9}$$

where T_d is the torque exerted on the disk. Provided that

[5] The first-order $m = 0$ terms are an exception. They should be combined into a single component proportional to $\cos(\kappa_p t)$, formally implying an infinite pattern speed. More on this is in the discussion section.

[6] In this paper we consider potential components only up to first order in e_p.

TABLE 1
NINE RESONANCES FOR A GIVEN VALUE OF m

Potential	Pattern Speed, $\Omega_{l,m}$	Torque, T_d Name	Torque, T_d Sign	Keplerian Position	Effects a_p	Effects e
$\phi_{m,m}$ principal.....	Ω_p	$T^{\rm OLR}_{m,m}$	+	$a_p(1 + 2/3\,m)$	⇓	↑
		$T^{\rm CR}_{m,m}$	?	a_p	?	?
		$T^{\rm ILR}_{m,m}$	−	$a_p(1 - 2/3\,m)$	⇑	↓
$\phi_{m-1,m}$ first-order	$\Omega_p - \kappa_p/m$	$T^{\rm OLR}_{m-1,m}$	+	$a_p(1 + 4/3\,m)$	↓	⇑
		$T^{\rm CR}_{m-1,m}$	(−)	$a_p(1 + 2/3\,m)$	(↑)	(⇓)
		$T^{\rm ILR}_{m-1,m}$	−	a_p	↑	↓
$\phi_{m+1,m}$ first-order.....	$\Omega_p + \kappa_p/m$	$T^{\rm OLR}_{m+1,m}$	+	a_p	↓	↓
		$T^{\rm CR}_{m+1,m}$	(+)	$a_p(1 - 2/3\,m)$	(↓)	(⇓)
		$T^{\rm ILR}_{m+1,m}$	−	$a_p(1 - 4/3\,m)$	↑	⇑

NOTE.—Up and down arrows denote whether T_d increases or decreases a_p and e_p. Leading terms, assuming a clean gap in a Keplerian disk, are distinguished by double arrows. Parentheses denote a dependence on $d(\Sigma/B)/dr$, with the sign appropriate to Σ/B decreasing toward the planet.

the unperturbed disk is circular, $e_d = 0$, equation (5) applied to the disk material on which the torque T_d is applied yields

$$\left(\Omega_{l,m} - \Omega_d\right) T_d = \frac{\Omega_d H_d}{2} \frac{de_d^2}{dt} \geq 0 \ . \tag{10}$$

Equality applies if the epicyclic motion of the disk material is not excited. Thus, a potential component may be viewed as transporting angular momentum from higher to lower angular velocity (Lynden-Bell & Kalnajs 1972). Consequently, $T_d > 0$ at an OLR and $T_d < 0$ at an ILR.

Because $\Omega_{l,m} - \Omega_d = 0$ at a corotation resonance, the sign of the corotation torque depends on whether the interaction is dominated by material inside or outside corotation. A simple understanding can be obtained by considering the behavior of collisionless particles. Disk particles close to the resonance experience slowly varying torques proportional to $\sin[m(\theta - \Omega_{l,m}t)]$, which change their orbital radii. Particles spiraling toward corotation drift at a decreasing rate with respect to the phase of the potential. The opposite pertains to particles moving away from corotation. As a result, there is a flux of particles toward corotation on both sides of the resonance. Material outside corotation loses angular momentum and that inside gains it. The corotation torque depends on the difference and is proportional to $-d(\Sigma/B)/dr$. Oort's constant, $B = (2r)^{-1} d(r^2\Omega)/dr$, which is equal to $\Omega/4$ for Keplerian rotation, appears because the radial drift rate is equal to the torque divided by $2B$. Epicyclic motions in particle disks and pressure in gas disks, neglected here but accounted for later, spread the region of influence over a radial width which for a Keplerian disk is comparable to the disk's vertical scale height. However, they do not affect the net corotation torque. The corotation torque, as described here, is transient. A discussion of the relation between its initial and steady-state values is given in § 6

We note that the corotation torque is negative if material outside the resonance dominates the interaction. This might appear surprising in light of our finding, based on the Jacobi constant, that torques at Lindblad resonances transfer angular momentum from higher to lower angular velocity. Wouldn't a similar conclusion apply to corotation resonances? The answer is no, but for a subtle reason. In evaluating the Jacobi constant near a Lindblad resonance we neglect the planet's perturbation potential in the energy budget. That is fine there, but it is not appropriate near a corotation resonance.

3.2. *Understanding the Effects of Resonances on the Eccentricities*

Angular momentum and energy transferred to the disk at a resonance is removed from the planet's orbit. Consequently,

$$\frac{dE_p}{dt} = \Omega_{l,m} \frac{dH_p}{dt} = -\Omega_{l,m} T_d \ . \tag{11}$$

An alternate derivation proceeds from the fact that the linear density perturbation at a resonance rotates with the pattern speed. Thus, the perturbed disk's gravitational back-reaction on the planet preserves the planet's Jacobi constant. Combining equations (5) and (11), we find

$$e_p \frac{de_p}{dt} = \left[\left(1 - e_p^2\right)^{-1/2} \Omega_p - \Omega_{l,m}\right] \frac{H_p^2 T_d}{(GM_*)^2 M_p^3} \ . \tag{12}$$

At first-order resonances $\Omega_{l,m} \neq \Omega_p$, so to lowest order in e_p,

$$e_p \frac{de_p}{dt} = \left(\Omega_p - \Omega_{l,m}\right) \frac{H_p^2 T_d}{(GM_*)^2 M_p^3} \ . \tag{13}$$

For first-order Lindblad resonances, we make use of equation (10) to prove that

$$\mathrm{sgn}\left(\frac{de_p}{dt}\right) = \mathrm{sgn}\left[(\Omega_p - \Omega_{l,m})(\Omega_{l,m} - \Omega_d)\right] \ . \tag{14}$$

Thus, e_p decreases if the resonance resides on the same side of corotation as the planet, and increases if it resides on the opposite side. Henceforth we adopt the terminology "coorbital"[7] and "external" to distinguish these two classes of first-order Lindblad resonances.

For first-order corotation resonances the sign of the torque is opposite to the sign of $d(\Sigma/B)/dr$. Therefore,

$$\mathrm{sgn}\left(\frac{de_p}{dt}\right) = \mathrm{sgn}\left[(\Omega_{l,m} - \Omega_p) \frac{d}{dr}\left(\frac{\Sigma}{B}\right)\right] \ . \tag{15}$$

If the planet has cleared a gap, the density increases away from it, so both first-order corotation resonances cause e_p to decay.

Next we examine how the principal Lindblad resonances affect the planet's eccentricity. Since $\Omega_{m,m} = \Omega_p$, we retain the lowest order dependence on e_p in equation (12), which reduces to

$$\frac{1}{e_p}\frac{de_p}{dt} = \frac{\Omega_p H_p^2 T_d}{2(GM_*)^2 M_p^3} \ . \tag{16}$$

Goldreich & Tremaine (1980) compare the rates at which the principal and first-order Lindblad resonances of the same m change the planet's eccentricity. They find that the former is smaller than the latter by a factor m, although both have the same dependence on e_p. We offer some additional comments. Because T_d is negative at an ILR and positive at an OLR, the effect of the principal Lindblad resonances on de_p/dt suffers from the same cancellation as their effect on da_p/dt. Rates of change of eccentricity and semimajor axis due to principal Lindblad resonances satisfy

$$\frac{4}{e_p}\frac{de_p}{dt} = -\frac{1}{a_p}\frac{da_p}{dt} \ . \tag{17}$$

After a planet clears a gap it migrates inward as the disk accretes, so its eccentricity increases. But since the timescale for eccentricity change is 4 times that for radial migration, principal Lindblad resonances are of negligible importance in eccentricity evolution.

3.3. *Comparison of Timescales*

Now we compare the timescale for eccentricity change, t_e, with that for semimajor axis migration, $t_{\rm vis}$. The semimajor

[7] In a Keplerian disk these resonances overlap the planet's semimajor axis.

axis of a planet that opens a gap evolves with the disk on the viscous timescale

$$t_{\rm vis}^{-1} \sim \frac{\nu}{r^2} \sim \alpha\Omega\left(\frac{h}{r}\right)^2 . \tag{18}$$

Here α is the standard viscosity parameter for accretion disks, and $h \approx c_s/\Omega$ is the vertical thickness of the disk, with c_s the sound speed. The planet's orbital eccentricity changes on the timescale

$$t_e^{-1} \equiv \frac{1}{e_p}\left|\frac{de_p}{dt}\right| \approx \left(\frac{r}{w}\right)^4 \left(\frac{M_p \Sigma r^2}{M_*^2}\right)\Omega , \tag{19}$$

where w is the gap's width. Equation (19), adapted from Goldreich & Tremaine (1980), is obtained by summing contributions to de_p/dt from first-order resonances within a narrow ring separated from the planet's position by an empty gap. Assuming Keplerian rotation, they find that e_p decays. However, damping by corotation resonances exceeds driving by Lindblad resonances by only a small margin, 4.6%. The timescale quoted above for eccentricity change is that due to either corotation or Lindblad resonances acting separately. Conditions under which this, rather than the net contribution from both types of resonance, is the appropriate t_e to compare with $t_{\rm vis}$ are described in § 6. To elucidate the comparison between t_e and $t_{\rm vis}$, we relate w to α and M_p/M_* by balancing the viscous torque[8]

$$T_{\rm vis} = 3\pi\nu\Sigma\Omega r^2 = 3\pi\alpha\Sigma r^2(\Omega h)^2 , \tag{20}$$

with the torque from the principal Lindblad resonances,

$$T_{\rm L} \approx \left(\frac{r}{w}\right)^3 \Sigma r^2 (r\Omega)^2 \left(\frac{M_p}{M_*}\right)^2 , \tag{21}$$

to obtain

$$\frac{w}{r} \approx (3\pi\alpha)^{-1/3}\left(\frac{r}{h}\frac{M_p}{M_*}\right)^{2/3} . \tag{22}$$

Our typical parameters, $\alpha = 10^{-3}$, $h/r = 0.04$, $M_p/M_* = 10^{-3}$, give $w \approx 0.4r$. Substituting this expression for w into equation (19) yields

$$t_e^{-1} \approx \frac{r}{w}\frac{\Sigma r^2}{M_p} t_{\rm vis}^{-1} . \tag{23}$$

For $w/r \approx 1$, eccentricity evolves faster than the semimajor axis provided that the disk is more massive than the planet.

Co-orbital Lindblad resonances can be ignored in investigations of the eccentricities of the orbits of shepherd satellites and narrow planetary rings because the surface density at the orbit of the shepherd satellite is negligible. But because the ratio of vertical thickness to orbital radius is so much larger in protoplanetary disks, $h/r \sim 0.04$, than in planetary rings, $h/r \lesssim 10^{-6}$, even a massive planet may not clear a very clean gap, so interactions at co-orbital Lindblad resonances could be significant. As shown by equation (14), these interactions damp the planet's orbital eccentricity. Attempts to estimate the rate at which first-order co-orbital Lindblad resonances damp eccentricity are described by Ward (1988) and Artymowicz (1993a). The latter concludes that, in a disk of uniform surface density, they damp eccentricity about 3 times faster than external first-order Lindblad resonances excite it.

[8] As written below, $T_{\rm vis}$ is appropriate to a Keplerian disk. More generally, the factor of 3 should be replaced by $(2B)^{-1}|r\,d\Omega/dr|$.

An apsidal resonance is a first-order inner Lindblad resonance with $l = 0$ and $m = 1$. Its pattern speed is equal to the planet's apsidal precession rate, $\Omega_{0,1} = \Omega_p - \kappa_p = \dot{\varpi}_p$. As a co-orbital first-order Lindblad resonance, it contributes to eccentricity damping. Application of the standard Lindblad resonance torque formula to the apsidal resonance led Ward & Hahn (1998, 2000) to conclude that an apsidal resonance damps eccentricity much faster than external first-order Lindblad resonances excite it.

We have described three types of resonant planet-disk interactions that damp eccentricity and one that excites it. In what follows we argue that eccentricity can grow provided that its initial value exceeds some minimal threshold and the planet clears a sufficiently clean gap. A minimal initial eccentricity is necessary for the nonlinear saturation of corotation torques. This involves a reduction of the surface density gradient at the resonance position. A clean gap renders ineffective damping by first-order co-orbital Lindblad resonances. Although damping due to the apsidal resonance might appear to be the most potent of all, it is likely to be unimportant. Apsidal waves have such long wavelengths in protoplanetary disks that they do not propagate. Thus, torques at apsidal resonances are much smaller than predicted by the standard Lindblad resonance torque formula.

4. APSIDAL RESONANCES

Apsidal resonances are located where the planet's apsidal precession rate matches that of the disk. They are special in a number of ways. The Doppler-shifted forcing frequency detunes more gradually from the epicyclic frequency with distance away from an apsidal resonance than it does at other Lindblad resonances. Thus the standard Lindblad resonance torque formula predicts that the apsidal torque

$$T_{0,1}^{\rm ILR} \sim -e_p^2\left(\frac{M_p}{M_*}\right)^2 \frac{\Sigma r^8\Omega^2}{(\Delta r)^4}\frac{\Omega}{r|d\dot{\varpi}_d/dr|} , \tag{24}$$

is larger by $\Omega/|\dot{\varpi}_d| \gg 1$ than that at an ordinary first-order Lindblad resonance separated by a distance $\Delta r \lesssim r$ from the planet's orbit (Goldreich & Tremaine 1978; Ward & Hahn 1998, 2000). For the same reason, apsidal waves have longer wavelengths than those at ordinary Lindblad resonances.

The derivation of the standard torque formula rests on the assumptions that the density waves are excited at Lindblad resonances, propagate away, and dissipate before reflecting. Because of their long wavelengths, apsidal waves in protoplanetary disks are not subject to the nonlinear steepening and shock dissipation that is the leading form of damping for density waves generated at ordinary Lindblad resonances (Goodman & Rafikov 2001). Instead, they are better viewed as standing waves trapped inside cavities, with viscous dissipation being their principal source of damping.

Provided the damping is light, each standing wave is characterized by an almost constant circulating angular momentum luminosity. We refer to this feedback cycle as a loop. The apsidal torque just compensates for the integrated damping around the loop. Thus the damping factor, defined as the ratio of the apsidal torque to the circulating angular momentum luminosity, is given by

$$\mathscr{F}_D = \oint dr\frac{\nu k^2}{v_g} \ll 1 . \tag{25}$$

If the cavity is not resonant, the circulating luminosity is similar to that which would be radiated in the absence of reflections. In this case, the damping factor is the appropriate reduction factor to apply to the torque calculated on the assumption that the apsidal wave propagates without reflection.

Another consequence of their long wavelengths is that apsidal waves experience significant off-resonance driving at gap edges. Off-resonance driving is crucial because the location, and even the existence, of an apsidal resonance associated with an embedded planet is sensitive to disk parameters.

In the reminder of this section we show that the standard formula considerably overestimates the apsidal torque. We begin by exploring the parameter space through estimates of disk and planet precession rates. Next, we provide a semiquantitative analysis of wave excitation at gap edges. We introduce coupling factors, $\mathscr{F}_C$, which are correction factors to the standard torque formula associated with edge driving as compared to that at resonance. Subsequently, we evaluate contributions to the apsidal torque made by various wave loops. For that, we combine the modest coupling factors, $\mathscr{F}_C$, with the more significant damping factors due to cavity feedback, $\mathscr{F}_D$. This is done separately for disks dominated by pressure and by self-gravity, and is summarized in Table 2.

4.1. *Precession Rates*

Forces due to pressure and self-gravity cause apsidal precession of the disk.[9] The disk's gravity alone determines the precession rate of the planet. Contributions to $\dot{\varpi}_d$ from pressure and self-gravity are of the order of

$$\dot{\varpi}_{d,\mathrm{pr}} \sim +\left(\frac{h}{r}\right)^2 \Omega \,, \tag{26}$$

and

$$\dot{\varpi}_{d,\mathrm{sg}} \sim -\frac{M_d}{M_*}\Omega \,, \tag{27}$$

respectively. Note that self-gravity gives rise to retrograde precession. The ratio of these contributions is of the order of

$$\left|\frac{\dot{\varpi}_{d,\mathrm{sg}}}{\dot{\varpi}_{d,\mathrm{pr}}}\right| \sim \frac{M_d}{M_*}\left(\frac{r}{h}\right)^2 \sim k_c r \equiv \frac{\pi G \Sigma r}{c_s^2} \,. \tag{28}$$

We therefore define pressure-dominated disks as disks with $k_c r \ll 1$ and self-gravity–dominated disks as those with $k_c r \gg 1$. Our standard parameters of $M_d/M_* = 10^{-2}$ and $h/r = 0.04$ yield $k_c r \cong 6$, just slightly in the self-gravity regime.

A planet with semimajor axis a_p, located in a gap of width $w \lesssim a_p$, precesses in a prograde fashion at a rate

$$\dot{\varpi}_p \sim +\frac{M_d}{M_*}\frac{a_p}{w}\Omega \,, \tag{29}$$

independent of the gas pressure.

4.2. *Apsidal Dispersion Relation*

Our reasoning is based on the WKBJ dispersion relation

$$(\omega - m\Omega)^2 = k^2 c^2 + \kappa^2 - 2\pi G|k|\Sigma \,, \tag{30}$$

although the long wavelengths of apsidal waves render it of marginal applicability. A more complete treatment would be based on analysis of global modes along the lines of Lee & Goodman (1999), Ogilvie (2001), Tremaine (2001), and Papaloizou (2002).

A simplified dispersion relation suitable for apsidal waves in the dual limits $\omega = \dot{\varpi}_p \ll \Omega$ and $|\dot{\varpi}_d| \ll \Omega$ reads

$$2\Omega(\dot{\varpi}_p - \dot{\varpi}_d) = \left(2\frac{k_c}{|k|} - 1\right)k^2 c_s^2 \,. \tag{31}$$

The radial group velocity follows from the dispersion relation:

$$v_g \equiv \frac{d\dot{\varpi}_p}{dk} = -\frac{kc^2}{\Omega}\left(1 - \left|\frac{k_c}{k}\right|\right) \,. \tag{32}$$

In some applications we specialize to a model disk in which $\Sigma \propto r^{-3/2}$ and $c_s^2 \propto r^{-1/2}$. An advantage of this model is that $k_c r$ is constant.

4.3. *Wave Driving at Gap Edges*

Far from the driving region, the asymptotic amplitude of an externally forced wave is proportional to the product of

[9] We neglect gravitational forcing by the planet, since it is assumed to be much less massive than the disk.

TABLE 2

Coupling, Damping, and Torque Reduction Factors

Loop and Wave Type	Main Driving	Coupling Factor, $\mathscr{F}_C$	Damping Factor, $\mathscr{F}_D$	Torque Reduction Factor, $\mathscr{F}_C\mathscr{F}_D$
		Gravity-dominated Disk		
Inner, LW	ingoing LW, $\lambda \approx$ w	$(w/a_p)^2$	$(\alpha/k_c r)(a_p/w)^2\Lambda_1$	$2\alpha(k_c r)^{-1}\Lambda_1$
Outer, LW+SW	outgoing LW, $\lambda \approx w$	$(w/a_p)^2$	$4\pi N\alpha$	$8\alpha k_c r(w/a_p)^2\Lambda_2$
Inner, SW	ingoing SW, $\lambda < w$	$1/(k_c r)^2$	$4\pi N\alpha$	$4\alpha(k_c r)^{-1}\Lambda_3$
		Pressure-dominated Disk		
Outer	outgoing, $\lambda \approx w$	$(w/a_p)^2$	$2\pi N\alpha$	$2\sqrt{2}\alpha(w/a_p)^2\Lambda_4$
Inner	ingoing, $\lambda \approx w$	$(w/a_p)^2$	$2\pi N\alpha$	$2\sqrt{2}\alpha(w/a_p)^2\Lambda_5$

Note.—Summary of coupling factors due to driving at a gap edge rather than to resonance, and damping factors due to viscous damping in a cavity as compared to radiative losses. The Λ are order unity factors that are given by $\Lambda_1 = 1 + 4(w/a_p) + 2(w/a_p)^2\ln(a_p/r_{\mathrm{in}})$, $\Lambda_2 = \ln(k_c r) + \ln(w/2a_p)$, $\Lambda_3 = \ln(a_p/r_{\mathrm{in}})$, $\Lambda_4 = \ln(w/a_p) - \ln(k_c r)$, and $\Lambda_5 = \ln(a_p/r_{\mathrm{in}})$.

the strength of the forcing and a characteristic net time over which it acts. The latter may be expressed as a characteristic length divided by the wave's group velocity in the forcing region. This characteristic length is the smaller of the wavelength and the distance over which the forcing decays (typically the distance to the perturber, e.g., w for a planet exciting waves at its gap's edges).

In the absence of reflections, the luminosity of the emitted wave is proportional to the group velocity times the absolute square of the asymptotic wave amplitude. For on-resonance driving, this leads to

$$L_H \propto \frac{\lambda_1^2}{v_g}\frac{\Omega}{r} , \tag{33}$$

where λ_1 is the first wavelength away from the resonance, and v_g is evaluated at a distance λ_1 from the resonance.[10] Note that this expression, which is equal to $(m-1)^{-1}$ for ordinary Lindblad resonances, is equal to $\Omega/(rd\dot{\varpi}/dr)$ for an apsidal resonance. This is the source of the apparently large apsidal torque given by equation (24).

Amplitudes of waves driven at edges are proportional to

$$L_H \propto \begin{cases} \dfrac{\lambda^2}{v_g}\dfrac{\Omega}{r} & \lambda \ll w, \\ \dfrac{w^2}{v_g}\dfrac{\Omega}{r} & \lambda \gg w. \end{cases} \tag{34}$$

We define the coupling factor, $\mathscr{F}_C$, for the luminosity of an edge-driven apsidal wave as the ratio between the expressions given by equation (34) for edge-driven waves and equation (33) for resonance driven waves. For ordinary density waves $\lambda \ll \lambda_1$ far from resonance so the coupling factor is small except close to resonance. However, an apsidal wave maintains a large wavelength throughout the disk, so its coupling factor is modest, except perhaps for short waves in a gravity-dominated disk.

4.4. *Pressure-dominated Disks*

The position of the apsidal resonance, r_*, obtained by equating equations (26) and (29), is

$$\frac{r_*}{a_p} \sim \frac{1}{k_c r}\frac{w}{a_p} . \tag{35}$$

For the wide gaps of interest to this investigation $r_* > a_p$. Equation (31) shows that apsidal waves are evanescent for $r > r_*$. The gap divides the region interior to r_* into two disconnected cavities. As shown in Figure 1, each cavity contains a wave loop composed of an outward-traveling leading wave and an inward-traveling trailing wave. Wave driving can occur either at a Lindblad resonance or at a disk edge. Both are present in the outer loop, but only the latter exists in the inner loop.[11]

An explicit calculation of the damping factor given by equation (25) is obtained with the aid of equation (32). Since $k_c \ll |k|$ in a pressure-dominated disk,

$$\mathscr{F}_D = 2\pi N\alpha , \tag{36}$$

[10] The factor Ω/r is included to make the expression dimensionless.

[11] We neglect driving at the inner and outer edges of the disk, since they are much more remote from the planet.

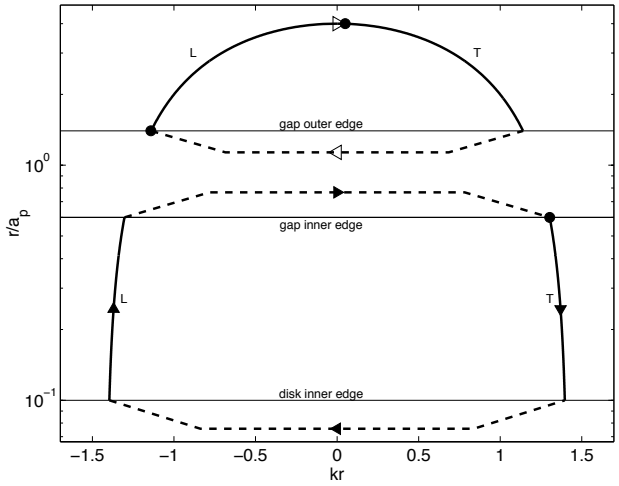

FIG. 1.—Apsidal cavities and their wave feedback loops in a pressure-dominated disk. The outer cavity is bounded by the outer edge of the gap and the resonance, while the inner cavity is bounded by the inner edge of the disk and the inner edge of the gap. Solid lines mark propagating waves in the cavities. Letters L and T denote leading and trailing waves, respectively. Reflections at gap edges, which interchange leading and trailing waves ($k \rightarrow -k$) are marked by dashed lines. Locations of wave driving are indicated by filled circles. The direction of wave propagation in the inner and outer loops is shown by filled and open triangles, respectively. Parameters chosen in constructing this figure are $w/r \approx 0.4$ and $k_c r = 0.1$. These place the apsidal resonance at $r_* \approx 4a_p$.

where N is the total number of wavelengths around the loop.

Next we estimate N. To do so, we calculate the apsidal wavelength from the *WKBJ* dispersion relation (eq. [31]). The first wavelength, λ_1, of an apsidal wave at resonance, defined by

$$\int_{r_*}^{r_*+\lambda_1} k(r)\, dr = 2\pi \tag{37}$$

yields

$$\lambda_1/r \approx (9\pi^2/2)^{1/3}(\Omega_d/\dot{\varpi}_d)^{1/3}(h/r)^{2/3} \approx 4 . \tag{38}$$

Well inside the resonance $\dot{\varpi}_d \gg \dot{\varpi}_p$, so the dispersion relation yields

$$\lambda/r = \sqrt{2}\pi(\Omega_d/\dot{\varpi}_d)^{1/2}(h/r) \approx 4 . \tag{39}$$

Our estimates of $\lambda/r \approx 4$ verify that apsidal waves are not pure traveling waves in a pressure-dominated disk. Equation (35) enables us to determine the number of wavelengths in each loop. They are

$$N = \begin{cases} (\sqrt{2}/\pi)\ln\left[(k_c r)^{-1}(a_p/w)\right] & \text{outer loop}, \\ (\sqrt{2}/\pi)\ln\left(a_p/r_{\rm in}\right) & \text{inner loop}. \end{cases} \tag{40}$$

Driving occurs at the gap edges as well as at the resonance. The coupling of the forcing to the waves is similar at all three sites because the values of v_g and k_r are. However, because of their proximity to the planet, the forcing is stronger at the gap edges than at the resonance. Consequently, we ignore wave driving at the resonance. Since the forcing decays over a scale $w \lesssim \lambda \approx r$, the circulating luminosity, which is equal to the radiated luminosity for an open cavity,

is smaller by the coupling factor $\mathscr{F}_C = (w/r)^2$ than that given by the standard torque.

Overall, the apsidal torque in a pressure-dominated disk is smaller by $\mathscr{F}_C\mathscr{F}_D = 2\pi N\alpha(w/r)^2$ than the value given by the standard torque formula given in equation (24).

4.5. *Self-Gravity–dominated Disks*

A planet does not have an apsidal resonance in a self-gravity–dominated disk because $\dot{\varpi}_d < 0$ and $\dot{\varpi}_p > 0$. However, it excites apsidal waves at the edges of the gap within which it orbits.

From the dispersion relation (eq. [31]), apsidal waves obey

$$|kr| = k_c r \pm \sqrt{(k_c r)^2 - 2k_c r\left(1 + \frac{\dot{\varpi}_p}{|\dot{\varpi}_d|}\right)} \cong \begin{cases} 2k_c r & \text{short waves,} \\ 1 + \dot{\varpi}_p/|\dot{\varpi}_d| \approx 1 + (r/a_p)(a_p/w) & \text{long waves.} \end{cases} \tag{41}$$

The two solutions for $|kr|$ describe four wave types because each solution allows for leading waves with $k < 0$ and trailing waves with $k > 0$. These four waves are depicted in Figure 2, which also shows their propagation directions as given by equation (32). Apsidal waves are evanescent outside the turning point at

$$\frac{r_{\rm tp}}{a_p} \approx \frac{w}{a_p}\left(\frac{1}{2}k_c r - 1\right), \tag{42}$$

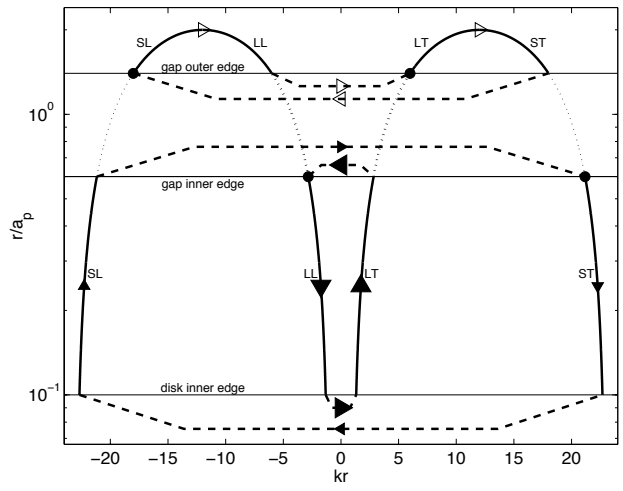

FIG. 2.—Apsidal cavities and their wave feedback loops in a self-gravity–dominated disk. The outer cavity is bounded by the outer edge of the gap and the resonance, while the inner cavity is bounded by the inner edge of the disk and the inner edge of the gap. Solid lines mark propagating waves. Letters SL, ST, LL, and LT denote short leading, short trailing, long leading, and long trailing waves, respectively. Reflections at gap edges, which interchange leading and trailing waves ($k \rightarrow -k$), are marked by dashed lines. The direction of wave propagation in the outer loop is marked by open triangles. In the long- and short-wave inner loops, the direction is given by large and small filled triangles, respectively. Locations of wave driving are marked by filled circles. Leakage between the different loops is possible at locations marked by dotted lines. It is significant for long waves (*heavy dotted lines*) and negligible for short waves (*light dotted lines*). Parameters chosen in constructing this figure are $w/r \approx 0.4$ and $k_c r \approx 12$. This places the turning point at $r_{\rm tp} = 2a_p$

where $v_g = 0$ and $k = k_c$. At the turning point, outgoing short leading waves reflect as long leading waves and outgoing long trailing waves reflect as short trailing waves. In drawing the figure we assume that $r_{\rm tp} > a_p$, as is appropriate for sufficiently wide gaps. Reflections at sharp edges of the disk material, which interchange leading and trailing waves, are indicated by dashed lines in the figure. These reflections form three wave feedback loops. One loop is contained in the outer cavity bounded by the outer edge of the gap and the turning point. The other two are contained in an inner cavity formed between the inner edges of the disk and the gap.

Apsidal waves are launched into the disk at gap edges. We identify four such launch points. We estimate the coupling factor, $\mathscr{F}_C$, for each launch point by following the procedure outlined in § 4.3. Since all apsidal waves have the same value of $|v_g| \sim k_c r(h/r)c_s$ in self-gravity–dominated disks, differences in their driving arise solely from differences in their wavelengths. At gap edges $kr \approx 1 + r/w$ for long waves and $kr \approx 2k_c r \gg 1$ for short waves.

Long waves, both inward leading and outward trailing, have $\lambda \approx w$ at gap edges, so their coupling factors are

$$\mathscr{F}_C = \left(\frac{w}{\lambda_1}\right)^2 \approx \left(\frac{w}{r}\right)^2. \tag{43}$$

Since short waves, both outward leading and inward trailing, have $\lambda \approx \pi/k_c$ at gap edges, their coupling factors are

$$\mathscr{F}_C = \left(\frac{\lambda}{\lambda_1}\right)^2 \approx \frac{1}{(k_c r)^2}. \tag{44}$$

Next we calculate the damping factor, $\mathscr{F}_D$, for each loop by applying equation (25).

Waves in the short wave inner loop maintain $kr \approx 2k_c r$. Therefore, the loop's damping factor can be written as

$$\mathscr{F}_D = 4\pi N\alpha. \tag{45}$$

In the long wave inner loop the long waves have $kr \approx 1 + (a_p/w)(r/a_p)$, so for it

$$\mathscr{F}_D \approx \frac{\alpha}{k_c r}\left(\frac{a_p}{w}\right)^2\left[1 + 4\left(\frac{w}{a_p}\right) + 2\left(\frac{w}{a_p}\right)^2 \ln\left(\frac{a_p}{r_{\rm in}}\right)\right]. \tag{46}$$

The outer loop has both long and short waves. The latter dominate the damping rate, which is given by

$$\mathscr{F}_D = 4\pi N\alpha, \tag{47}$$

where N is the number of short wavelengths in the outer loop;

$$N \approx \frac{2k_c r}{\pi}\ln\frac{r_{\rm tp}}{a_p}, \tag{48}$$

with $r_{\rm tp}/a_p$ given by equation (42). Thus, the outer loop's damping factor reads

$$\mathscr{F}_D \approx 8\alpha k_c r \ln\left(\frac{w}{2a_p}k_c r\right). \tag{49}$$

Finally, we discuss the leaking of waves across the gap. Leakage is a consequence of the disk's self-gravity and is substantial for waves whose wavelengths are comparable to

or larger than the gap width. Thus, it strongly couples the outer loop to the inner long wave loop. Waves driven in latter are likely to be mainly dissipated in the former.

4.6. *Overall Importance of Apsidal Waves*

We have shown that the apsidal torque in protoplanetary disks is likely to be much smaller than the standard torque formula predicts. Now we compare the rate at which it damps a planet's orbital eccentricity to the rate at which torques at ordinary first-order external Lindblad resonances excite eccentricity.

To calculate the ratio of rates, we multiply the torque reduction factor, $\mathscr{F}_C\mathscr{F}_D$, by w/r to account for the r/w ordinary first-order resonances that lie within a distance $\sim w$ from the planet, and then by $\Omega/\dot{\varpi}$, the ratio of the standard apsidal torque to the torque at an ordinary first-order Lindblad resonance. The result is approximately $6\alpha(w/r)^3(r/h)^2$ for both pressure- and self-gravity–dominated disks. For an equilibrium gap it simplifies, with the aid of equation (22), to

$$0.6\left(\frac{r}{h}\right)^4\left(\frac{M_p}{M_*}\right)^2 . \tag{50}$$

With parameters $M_p/M_* \approx 10^{-3}$ and $h/r \approx 0.04$, the apsidal torque is about a factor of 4 smaller than that at ordinary Lindblad resonances at the gap edge. So far, we have implicitly assumed that the wave forcing strength at an apsidal resonance is comparable to that at an ordinary first-order Lindblad resonance. However, closer examination reveals that it is smaller by

$$\frac{(D_\beta - 2)\left(1 - \beta D_\beta\right)b^1_{1/2}(\beta)}{(D_\beta - 2m)\left(2m - 1 - \beta D_\beta\right)b^m_{1/2}(\beta)} , \tag{51}$$

where $b^m_{1/2}$ is a Laplace coefficient, $m = (1 + \beta^{-3/2})/(1 - \beta^{-3/2})$, and $D_\beta \equiv \partial/\partial\beta$. The ratio of the apsidal to ordinary Lindblad torque depends on the square of the forcing strength, a factor which increases from ≈ 0.035 for $w/r \ll 1$ to ≈ 0.14 for $w/r = 0.4$. Thus, with our standard parameters, eccentricity damping by the apsidal torque is probably even slower than that which results from the close competition between eccentricity damping by unsaturated corotation resonance torques and eccentricity excitation by ordinary external Lindblad resonance torques. However, given the sensitivity of equation (50) to the planet's mass and the disk's thickness, and the fact that its derivation is based on the marginally valid WKBJ approximation, this is not a conclusive result.

In our discussions of both the pressure-dominated and self-gravity–dominated disks we have deliberately glossed over the issue of the cavity size measured in wavelengths. Our estimate of torque reduction assumes that the amplitude of the standing wave inside its cavity is comparable to that which a traveling wave would have in the absence of a reflecting boundary. This would be an underestimate for a cavity tuned near resonance.

4.7. *Buildup of the Feedback Loop*

If it occurs, eccentricity growth due to planet-disk interactions would result from instability.[12] Suppose a planet acquires a small orbital eccentricity. Initially, its apsidal wave cavities will be empty. Each cavity will then fill to equilibrium on a timescale

$$t_g = \oint dr/v_g . \tag{52}$$

As this happens, apsidal waves will be radiated into the cavity at a rate given by $\mathscr{F}_C T^{\rm ILR}_{0,1}$. After equilibrium is attained, the cavity will be filled with *negative* angular momentum. This will result in an increase of the planet's angular momentum at nearly fixed energy.[13] But an increase of the planet's angular momentum by ΔH_p at fixed energy implies a decrease of it's orbital eccentricity according to

$$M_p a_p^2 \Omega_p \Delta e_p^2/2 \approx -\Delta H_p . \tag{53}$$

Thus the ratio, $\mathscr{R}$, of $t_g\mathscr{F}_C T^{\rm ILR}_{0,1}$ to $M_p a_p^2 \Omega_p e_p^2/2$ measures the importance of the stored angular momentum on the initial eccentricity.[14]

Next we estimate this ratio for both pressure- and gravity-dominated disks. In each of our models, the apsidal wave group is nearly independent of radius for all waves (except very close to resonance or turning points). Therefore, the major contribution to the numerator comes from the outer loop. The length of that loop is given by the resonance position in a pressure-dominated disk (eq. [35]), and by the location of the turning point in a self-gravity–dominated disk (eq. [42]). Making use of equation (32) for the group velocity, as well as the precession rates given by equations (26) and (27), we find that

$$\mathscr{R} \approx k_c r (M_p/M_d)(a_p/w) \tag{54}$$

applies to both pressure- and self-gravity–dominated disks. For pressure-dominated disks, unless the gap is very narrow, this is guaranteed to be less than unity, since pressure-dominated disks have $k_c r < 1$ and we assume that $M_p < M_d$. In addition, this should be further reduced by the abnormally small forcing of the apsidal wave, as discussed following equation (51). For a self-gravity–dominated disk, the result is more marginal, and for sufficiently large $k_c r$ indeed $\mathscr{R} > 1$.

If $\mathscr{R} < 1$, as is the case for pressure-dominated disks, and also for moderately self-gravity–dominated disks, such as the disk with our standard parameters, the angular momentum stored in the loop is negligible. Steady state between the planet and its cavities is obtained without significant decrease of the planet's eccentricity. For $\mathscr{R} > 1$, the planet's initial eccentricity would have been reduced by a factor of $\sqrt{R}$ during the filling of its apsidal cavities.

We end by noting that close to gap edges, the disk acquires an eccentricity of the order of $e_d = (M_p/M_d)\times(a_p/w)e_p$. Should this ratio $(M_p/M_d)(a_p/w)$ approach unity, the forcing of apsidal waves would be drastically reduced, rendering the apsidal torque impotent.

5. LINDBLAD AND COROTATION RESONANCES

First-order Lindblad resonances are of two kinds, external ones which excite the planet's eccentricity, and co-orbital ones which damp it. In a disk of uniform surface

[12] As we show later, it is finite amplitude instability that is at issue.

[13] The ratio of energy to angular momentum carried by apsidal waves is $\dot{\varpi}_p/\Omega_p \ll 1$.

[14] This ratio is independent of e_p.

density, damping by co-orbital resonances is about a factor of 3 faster than excitation by the external ones (Artymowicz 1993a). Obviously, damping due to co-orbital resonances is weaker if the planet orbits within a gap. However, surface density gradients associated with a gap activate eccentricity damping by corotation resonances. Can a gap be clean enough to prevent eccentricity damping by co-orbital Lindblad resonances, yet have sufficiently shallow density gradients so as to avoid eccentricity damping by corotation resonances? Although we have not been able to answer this question in general, the two examples described below suggest that it is not possible.[15]

Here we compare the rate of eccentricity damping by co-orbital Lindblad resonances plus corotation resonances with the rate of eccentricity excitation by external Lindblad resonances. Our analysis takes into account a gap in the surface density around the planet's orbit but assumes that this does not significantly perturb the Keplerian rotation rate. The location of the resonances in such disks is depicted on the left panel of Figure 3. For simplicity, we concentrate on the material external to the planet's orbit. In this region the external and co-orbital Lindblad resonances are outer and inner ones, respectively. We employ three constants, $\mathscr{C}_{\rm eLR}$, $\mathscr{C}_{\rm cLR}$, and $\mathscr{C}_{\rm CR}$, to describe the relative strengths of the external Lindblad resonances, the co-orbital Lindblad resonances, and the corotation resonances, respectively. As described in § 3, $\mathscr{C}_{\rm cLR}/\mathscr{C}_{\rm eLR} \approx 3$ and $\mathscr{C}_{\rm CR}/\mathscr{C}_{\rm eLR} = 1.046$. We take the torque cutoff to occur at $r_1 - a_p \sim h$ for each type of resonance (Goldreich & Tremaine 1980; Ward 1986; Artymowicz 1993b).

Eccentricity excitation by first-order external Lindblad resonances is evaluated from

$$\frac{1}{e_p}\frac{de_p}{dt}\Big|_{\rm eLR} = \int_{r_1}^{\infty} \frac{\mathscr{C}_{\rm eLR}}{(r-a_p)^5}\left[\frac{\Sigma(r)}{B_d}\right]dr \,. \tag{55}$$

[15] In this section we neglect possible saturation of corotation resonances.

A similar expression describes eccentricity damping by first-order co-orbital Lindblad resonances, except that Σ is evaluated at the planet's semimajor axis,

$$\frac{1}{e_p}\frac{de_p}{dt}\Big|_{\rm cLR} = -\int_{r_1}^{\infty} \frac{\mathscr{C}_{\rm cLR}}{(r-a_p)^5}\left[\frac{\Sigma(a_p)}{B_d}\right]dr = -\frac{\mathscr{C}_{\rm cLR}}{4(r_1-a_p)^4}\frac{\Sigma(a_p)}{B_d} \,. \tag{56}$$

The effect of corotation resonances on eccentricity evolution is given by

$$\frac{1}{e_p}\frac{de_p}{dt}\Big|_{\rm CR} = -\int_{r_1}^{\infty} \frac{\mathscr{C}_{\rm CR}}{4(r-a_p)^4}\frac{d}{dr}\left[\frac{\Sigma(r)}{B_d}\right]dr \,. \tag{57}$$

Integrating by parts, we arrive at

$$\frac{1}{e_p}\frac{de_p}{dt}\Big|_{\rm CR} = -\int_{r_1}^{\infty} \frac{\mathscr{C}_{\rm CR}}{(r-a_p)^5}\left[\frac{\Sigma(r)}{B_d}\right]dr + \frac{\mathscr{C}_{\rm CR}}{4(r_1-a)^4}\frac{\Sigma(r_1)}{B_d} \,. \tag{58}$$

Except for the negative sign and the substitution of $\mathscr{C}_{\rm CR}$ for $\mathscr{C}_{\rm eLR}$, the first term is identical to that for external Lindblad resonances. The second term, which is positive, may be viewed as a correction due to disk material close to the planet's orbit.

Equations (55), (56), and (58) combine to yield

$$\frac{1}{e_p}\frac{de_p}{dt} = -\int_{r_1}^{\infty} \frac{(\mathscr{C}_{\rm CR}-\mathscr{C}_{\rm eLR})}{(r-a_p)^5}\left[\frac{\Sigma(r)}{B_d}\right]dr - \frac{\mathscr{C}_{\rm cLR}\Sigma(a_p) - \mathscr{C}_{\rm CR}\Sigma(r_1)}{4(r_1-a_p)^4 B_d} \,. \tag{59}$$

If the planet clears a sufficiently clean gap, only the first term survives, and eccentricity damping by corotation resonances overcomes eccentricity driving by external Lindblad resonances, but only by a small margin, since

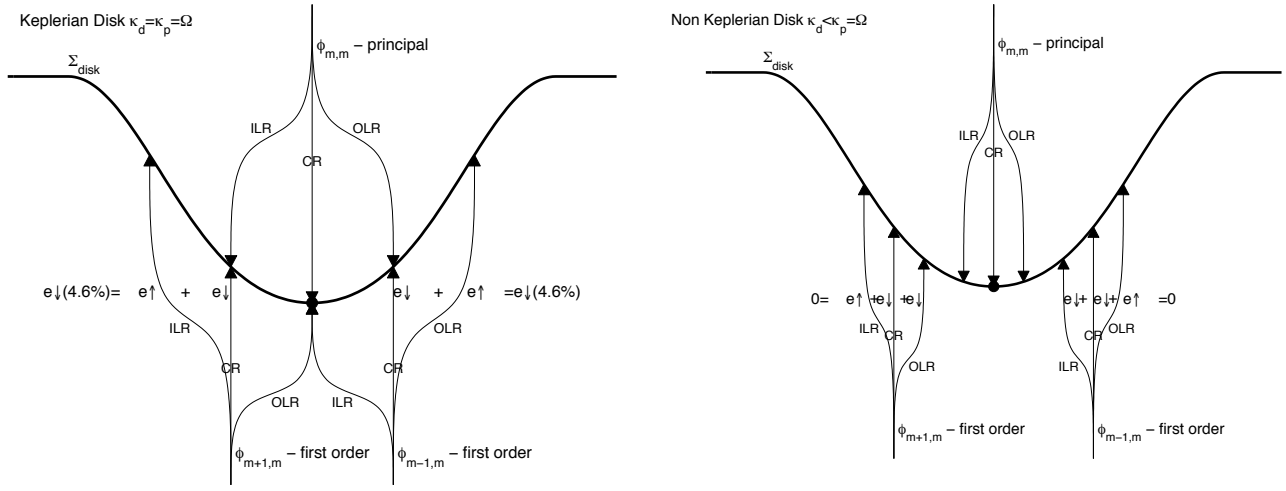

FIG. 3.—Location of resonances in a Keplerian disk (*left*), and in a low epicyclic frequency disk, $\kappa_d/\Omega_d \ll 1$ (*right*). The planet's motion is assumed to be Keplerian, $\kappa_p = \Omega_p$. The smaller κ_d/Ω_d is, the closer the principal Lindblad resonances are to the gap's center. Competition between eccentricity excitation and damping is tight in each case. For a Keplerian disk with a clean gap, the competition is between the external Lindblad resonances which excite eccentricity and corotation resonances which damp it. With decreasing epicyclic frequency, the co-orbital and external Lindblad resonances approach each other. Their effects nearly cancel, leaving a small residual eccentricity growth rate which is more completely canceled by the corotation resonances.

$\mathscr{C}_{\rm CR}/\mathscr{C}_{\rm eLR} = 1.046$.[16] Residual material in the gap leads to additional eccentricity damping unless $\Sigma(a_p)/\Sigma(r_1) < \mathscr{C}_{\rm CR}/\mathscr{C}_{\rm cLR} \approx \frac{1}{3}$. However, such a steep density gradient near the center of the gap is incompatible with our assumption that the disk maintains Keplerian rotation.

Next we examine how departures from Keplerian rotation might affect the balance between eccentricity driving and damping. Gas pressure perturbs the disk's epicyclic frequency. It decreases κ_d at the outskirts of a gap and increases it around the middle.[17] Provided that the gap is sufficiently clean, only resonances in its outer parts need be considered. Numerical simulations of gap formation by planets show that this limit can be achieved, at least in two-dimensional disks. This requires $1 \ll |d^2 \ln \Sigma/d \ln r^2| \lesssim (r/h)^2$. The upper limit is set by the requirements that principal Lindblad resonances are located away from the planet's semimajor axis and by the Rayleigh stability criterion. It motivates us to investigate the eccentricity evolution of a planet that resides in a gap where the epicyclic frequency is much smaller than the orbital angular velocity.

As $\kappa_d/\Omega_d \to 0$, $d\Omega_d/dr \to -2\Omega_d/r$, and the positions of the inner and outer Lindblad resonances associated with a given $\phi_{m-1,m}$ potential component approach, from opposite sides, the location of the corresponding corotation resonance (see right panel of Fig. 3). This simplifies comparison of the influences of the different resonances on eccentricity evolution. Inserting these approximations into the expressions for the torques at first-order resonances given by Goldreich & Tremaine (1979), we obtain

$$T^{\rm CR}_{m-1,m} \approx -\frac{m\pi^2\phi^2_{m-1,m}r}{\kappa_d^2}\frac{d\Sigma}{dr} \tag{60}$$

and

$$T^{\rm OLR,\,ILR}_{m-1,m} \approx \pm\frac{m^2\pi^2\phi^2_{m-1,m}\Sigma}{\kappa_d^3/\Omega} \ . \tag{61}$$

Note that in the limit $\kappa_d/\Omega_d \to 0$, each Lindblad torque dominates the corotation torque. However, the Lindblad torques have opposite signs, and when summed making use of their separations $\mp r\kappa_d/2m\Omega_d$, we discover that

$$T^{\rm ILR}_{m-1,m} + T^{\rm OLR}_{m-1,m} = \frac{m\pi^2\phi^2_{m-1,m}r}{\kappa_d^2}\frac{d\Sigma}{dr} \ . \tag{62}$$

So to leading order, the torques at the inner and outer Lindblad resonances just cancel that at the corotation resonance, implying $de_p/dt = 0$.

To summarize, neither of our examples yields a prediction of eccentricity growth. For Keplerian rotation, eccentricity damping by corotation resonances is slightly faster than eccentricity excitation by external Lindblad resonances. In the extreme limit of vanishing epicyclic frequency, eccentricity damping by corotation and co-orbital Lindblad resonances just balances eccentricity driving by external Lindblad resonances.

[16] This situation pertains to narrow planetary rings and their shepherd satellites (Goldreich & Tremaine 1980).

[17] For an isothermal gas the leading correction to κ_d^2 is proportional to the second radial derivative of the logarithm of the surface density.

6. SATURATION OF COROTATION RESONANCES

6.1. *Particle Disk*

We focus on the motion of the guiding center of a particle's orbit as measured in the corotation frame. A guiding center displaced by $|a - a_c|$ from corotation drifts at an unperturbed rate

$$\left|\frac{d\theta}{dt}\right| \sim \Omega\frac{|a-a_c|}{a_c} \ . \tag{63}$$

To first order in ϕ, it oscillates radially with velocity,

$$\frac{da}{dt} \sim \frac{m\phi}{\Omega a_c} \ , \tag{64}$$

at a frequency

$$\omega \sim m\Omega\frac{|a-a_c|}{a_c} \ . \tag{65}$$

The radial oscillation amplitude,

$$\Delta a \sim \frac{\phi}{\Omega^2|a-a_c|} \ , \tag{66}$$

equals $|a - a_c|$ for

$$|a_l - a_c| \sim \frac{\phi^{1/2}}{\Omega} \ . \tag{67}$$

Therefore, inside this boundary, the linear approximation fails. A guiding center located inside this boundary, known as a separatrix, circulates around the nearest potential maximum, an intrinsically nonlinear motion referred to as libration. The libration frequency declines from the small-amplitude value

$$\omega_l \sim \frac{m\phi^{1/2}}{r} \tag{68}$$

to zero at the separatrix.

6.1.1. *Torque Evolution in the Collisionless Limit*

Next we sketch how the corotation torque evolves following the application of the potential at $t = 0$.[18] For $\omega_l t \ll 1$, $T_{\rm CR}$ has the standard value given by Goldreich & Tremaine (1979). The torque is exerted on particles whose guiding centers lie within

$$|a - a_c| \lesssim \frac{a_c}{m\Omega t} \ . \tag{69}$$

As $\omega_l t$ approaches and then increases beyond unity, T_c declines to zero. This occurs because the circulation of the guiding centers trapped within the libration zone erases the contribution their associated particles make to the gradient of Σ/B.

6.1.2. *Effect of Viscosity*

Next we suppose the disk is endowed with kinematic viscosity ν. Particles with guiding centers interior and exterior to the separatrix exchange on the viscous diffusion timescale

$$t_\nu \sim \frac{(a_l - a_c)^2}{\nu} \sim \frac{\phi}{\Omega^2\nu} \ . \tag{70}$$

Provided $\omega_l t_\nu \ll 1$, the steady state torque maintains its

[18] To limit the impulsive excitations of epicyclic motions, we assume that the potential is turned on slowly compared to Ω^{-1}.

standard value. In the opposite limit, $\omega_l t_\nu \gg 1$, it is reduced by saturation Goldreich & Tremaine (1981). The reduction factor is approximated by the fraction of guiding centers that are replaced in the libration timescale ω_l^{-1}, namely,

$$\frac{1}{\omega_l t_\nu} \sim \frac{r\nu\Omega^2}{m\phi^{3/2}} \ . \tag{71}$$

An equivalent way to view the saturation criterion is to compare the radial width, $\delta_\nu \sim (r\nu/m\Omega)^{1/3}$, of the viscous boundary layer surrounding corotation with the width of the libration zone, $\delta_l \sim \phi^{1/2}/\Omega$; $\delta_\nu/\delta_l \sim (\omega_l t_\nu)^{-1/3}$.

6.2. *Gas Disk*

Ogilvie & Lubow (2002) provide an elegant derivation of the steady-state torque in a three-dimensional gaseous disk with finite viscosity. It demonstrates that the saturation of corotation resonances in a gas disk is similar to that in a particle disk. This is not surprising. Libration zones similar to those in a particle disk are also present in a gas disk, because pressure has only a negligible effect on the zeroth-order azimuthal velocity (in the corotation frame) and the first-order radial velocity. Even the spreading of the corotation torque over a distance of the order of c_s/Ω in a gas disk has an analogous behavior in a particle disk. The steady torque in a particle disk is exerted on particles whose guiding centers fall within the narrower of the libration regions and the viscous boundary layer. However, these particles are distributed in a layer of width equal to their epicyclic radii.[19]

Ogilvie & Lubow (2002) show that the level of saturation can be expressed in terms of a single parameter, p, defined as the square of the ratio of the libration width to the viscous width:

$$p \equiv \left(\frac{-d\ln r}{d\ln\Omega}\right)\frac{\phi}{\kappa^2}\left(\frac{-m\,d\Omega/dr}{\nu}\right)^{2/3} \sim \left(\frac{m}{r_c\Omega^2\nu}\right)^{2/3}\phi \ . \tag{72}$$

For $p \ll 1$ the corotation torque is unsaturated, whereas for $p \gg 1$ it is reduced by a factor of the order of $p^{-3/2}$, in agreement with the expression given for a particle disk by equation (71).

Next we estimate p for the most important corotation resonances. These are located near the edge of the gap that the planet opens in the disk. Substituting into equation (72) the first-order potential $\phi_{m\pm1,m} \approx me(M_p/M_*)(r\Omega)^2$ along with the appropriate m for an equilibrium gap as given by equation (22), we arrive at

$$p_{\rm eq} \approx \left(\frac{r}{h}\right)^{2/9}\left(\frac{M_*}{M_p}\right)^{1/9}\frac{e_p}{\alpha^{1/9}} \equiv Se_p \tag{73}$$

Fortunately, the dependence of $p_{\rm eq}$ on poorly known parameters is weak. With our typical values, $S \approx 20$, so significant saturation, that is $p_{\rm eq} \approx 1$, is achieved for $e_p = 0.05$. A much smaller value would suffice to tip the balance from eccentricity damping by corotation resonances in favor of eccentricity driving by external Lindblad resonances.

Eccentricity evolution during steady-state gaps is then given by

$$\frac{1}{e_p}\frac{de_p}{dt} = \frac{1}{t_e}\left[1 - \frac{\mathscr{C}_{\rm CR}}{\mathscr{C}_{\rm eLR}}F(p_{\rm eq})\right] , \tag{74}$$

[19] We assume that c_s/Ω is larger than both the width of the libration region and the viscous boundary layer.

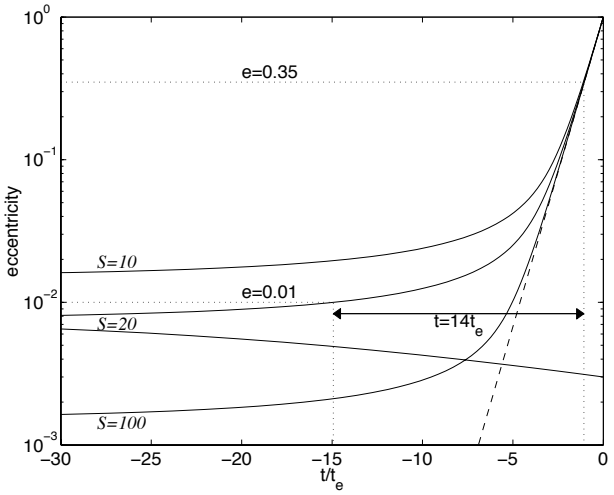

FIG. 4.—Eccentricity evolution with a partially saturated corotation resonance. The arbitrary time origin is chosen such that $e_p = 1$ at $t = 0$. Solid lines show how the eccentricity grows for three values of $S = 10$, 20, 100 with $\mathscr{C}_{\rm CR}/\mathscr{C}_{e,\rm LR} = 1.046$. These are to be compared to the dashed line, which illustrates eccentricity amplification under complete saturation. For $S = 20$ we also include a case illustrating the decay of a subcritical eccentricity. Dotted lines demonstrate that for $S = 20$ and partial saturation it takes about 14 Lindblad growth timescales for the eccentricity to increase from slightly above critical $e = 0.01$ to $e = 0.35$, whereas for complete saturation it would have taken only 3.6.

where $F(p)$ is the saturation function, which is numerically evaluated by Ogilvie & Lubow (2002) and can be interpolated as $F(p) \cong (1 + 0.65p^3)^{5/6}/(1 + 1.022p^2)^2$. Solutions of this equation for several values of S are given in Figure 4.

The above analysis assumes a steady-state gap and a steady-state saturation level. However, the initial value of e_p must survive damping until the torque is adequately saturated. This condition is satisfied provided that the timescale for eccentricity damping given by equation (19) is shorter than the libration timescale. This requires

$$e \gtrsim \alpha^{5/3}\left(\frac{h}{r}\right)^{10/3}\left(\frac{M_d}{M_*}\right)^2\left(\frac{M_p}{M_*}\right)^{-7/3} \sim 10^{-5} \ . \tag{75}$$

The width of the libration zone increases as the eccentricity grows. Libration zones from neighboring corotation resonances do not overlap, provided that

$$e_p \lesssim \left(\frac{M_p}{M_*}\right)^{7/3}\left(\frac{h}{r}\right)^{-10/3}\alpha^{-5/3} \approx 10 \ . \tag{76}$$

Further analysis is needed when this condition is violated.

The numerical values apply for our typical parameters. However, with our standard disk parameters but a lighter 0.1 M_J planet, overlap would occur for $e_p \sim 0.1$. It is plausible that overlap would limit corotation saturation and might therefore also limit eccentricity growth.

7. DISCUSSION

Resonant interactions between a planet and a protostellar disk cause the planet's orbital eccentricity to evolve on a short timescale. We have investigated whether these interactions might be responsible for the eccentric orbits that

characterize recently discovered extrasolar planets. Our preliminary findings are as follows.

Co-orbital Lindblad resonances damp eccentricity. They dominate the eccentricity evolution of planets that are too small to clear gaps (Ward 1988; Artymowicz 1993a). External Lindblad resonances excite eccentricity (Goldreich & Tremaine 1980). Lindblad resonances, by themselves, lead to net eccentricity excitation for planets which open clean gaps. However, gradients of surface density are enhanced in the walls of gaps, and these activate eccentricity damping by corotation resonances. Unsaturated corotation resonances damp eccentricity slightly faster than external Lindblad resonances excite it (Goldreich & Tremaine 1980). Corotation resonances saturate because fluid becomes trapped in libration zones around potential maxima. Saturation is effective if the libration timescale is shorter than that for viscous diffusion across the radial width of the libration zone. This requires the planet to obtain an initial orbital eccentricity of the order of 1%. Thus eccentricity growth due to planet-disk interactions is a finite-amplitude instability.

The excitation of apsidal waves results in eccentricity damping. Apsidal waves have longer wavelengths than other density waves. Standard density-wave theory formally implies that eccentricity damping due to apsidal waves is more potent than other forms of eccentricity change due to planet-disk interactions. However, because of their long wavelengths, apsidal waves are standing rather than traveling disturbances in protoplanetary disks. Unlike traveling waves, they do not steepen into shocks and dissipate, but instead are weakly damped by viscosity. As a result, the apsidal torque is much smaller than the standard torque formula predicts. Whether this reduction suffices to allow eccentricity growth depends sensitively on the thickness of the disk and the mass of the planet. Uncertainties in our calculations do not allow us to specify the exact values needed for eccentricity growth. However, growth is possible with reasonable parameters.

Next we provide a concrete example of a system in which eccentricity growth might occur. Suppose that a Jupiter mass planet with $M_p/M_* \approx 10^{-3}$, initial semimajor axis $a_p \approx 1$ AU, and initial eccentricity $e_p \approx 0.01$ is embedded in a protostellar disk with radius to scale high ratio $r/h \approx 25$ and viscosity parameter $\alpha \approx 10^{-3}$. The planet would open a wide gap with $w \approx r/2$. If the gap were as clean as the Rayleigh stability condition, $\kappa^2 > 0$, permits, the residual surface density at its center would be so small that eccentricity damping due to co-orbital Lindblad resonances would be negligible. Acting separately, either eccentricity damping by corotation resonances or eccentricity excitation by external Lindblad resonances would proceed on a timescale of the order of 10^5 yr. However, if the corotation resonances were unsaturated and they were acting together with the Lindblad resonances, eccentricity would damp on a significantly longer timescale. Given the initial eccentricity, partial saturation of the corotation resonances leading to eccentricity growth would occur on a libration timescale that is of the order of 200 yr, so eccentricity would not damp before saturation. A 1% eccentricity leads to a level of saturation marginally sufficient for eccentricity growth. As the eccentricity increases, so would the level of saturation, and thus the eccentricity growth rate. Figure 4 shows that the eccentricity could reach the observed mean value of $e_p = 0.35$ within about 1.5×10^6 yr.

Investigations of eccentricity evolution due to planet-disk interactions are plagued by several major uncertainties.

1. Angular momentum transport by internal stresses plays a major role in disk accretion, gap formation, and the saturation of corotation resonances. Presumably it arises from an instability, but we lack a basic understanding of its origin and character. At present, all we can do is assume that the disk possesses a kinematic α viscosity. Dissipation of disturbances near resonances occurs through shocks and turbulence. How these contribute to angular momentum transport is a subject for future investigation. Analogous phenomena are involved in maintaining sharp edges in planetary rings (Borderies, Goldreich, & Tremaine 1982a, 1982b).

2. Clean gaps are essential for the suppression of eccentricity damping by co-orbital Lindblad resonances. Two-dimensional simulations produce gaps of the requisite cleanliness, but it is not yet known whether three-dimensional simulations will confirm their reality (Bryden et al. 2000). The Rayleigh stability criterion, $\kappa^2 > 0$, limits the magnitude of density gradients in gap walls. There are also weaker, nonaxisymmetric instabilities that come into play at positive κ^2. Examining their role in determining gap shape is a task best suited to a coordinated attack by analytical calculations and numerical simulations.

3. Jovian mass planets should be able to open gaps in protostellar disks. Those that were not accreted onto and consumed by their central stars must have been present while the disk dispersed. During the latter stages of disk dispersal, they would have been more massive than the disk. It is known from studies of narrow planetary rings that the growth and damping of a ring's eccentricity is in most respects identical to that of the satellites which shepherd it (Goldreich & Tremaine 1980). The ratio of the rates of eccentricity change of ring and satellite are inversely proportional to the ratio of ring to satellite mass. To maintain an eccentric shape a narrow ring must precess rigidly. This requires the wavelength of the apsidal wave with pattern speed equal to the precessional angular velocity to be longer than the ring's radial width. Since apsidal waves in protostellar disks have wavelengths comparable to the local radius, large regions of these disks might maintain eccentric shapes.

4. Our proposal for eccentricity growth due to planet-disk interactions involves a finite-amplitude instability. However, we do not have an obvious candidate for giving a planet the requisite initial eccentricity of the order of 1%. Gravitational interactions with surface density perturbations created by instabilities in the walls of gaps is one possibility.

5. Once an adequate core has been assembled, the accretion of gas to form a Jovian mass planet proceeds rapidly. As its mass increases, a planet begins to clear a gap which hinders its ability to accrete additional gas. Eccentricity growth could occur prior to gap attaining its equilibrium width, provided that it becomes sufficiently clean. This would have two positive effects on the planet's potential for eccentricity growth. It would lessen the initial eccentricity required for adequate saturation of corotation resonances, since $e_{\rm crit} \propto w^{5/3}$ for fixed viscosity, and it would speed up the rate of eccentricity increase, since $de_p/dt \propto w^{-4}$.

6. The sites of first-order corotation resonances coincide with those of principal Lindblad resonances. Linear

perturbations associated with the latter are larger than those of the former by a factor of the order of $(me_p)^{-1}$. Whether this affects saturation of corotation resonances is an open issue.

7. We only consider principal and first-order resonances in this paper. While this is adequate for examining the excitation and damping of small eccentricities, higher order resonances will have to be taken into account if we want to examine the growth of eccentricity to the large values characteristic of extrasolar planets.

8. Hill radii of Jupiter-mass planets are larger than the vertical scale heights of protostellar disks. Thus, they might at least temporarily trap gas in quasi–two-dimensional horseshoe orbits. Then some of the angular momentum deposited at co-orbital Lindblad resonances could find its way back into the planet's orbit. This would reduce the eccentricity damping rate of co-orbital Lindblad resonances.

9. Our analysis is suitable for $m \gg 1$. However, for Jupiter-mass planets, and for $\alpha = 10^{-3}$, the size of the gap $w \approx r$ suggests $m \approx 1$. Significant corrections may apply in this limit; see, e.g., Artymowicz et al. (1991).

10. The first-order axisymmetric $m = 0$ resonance deserves special attention. It can be thought of as a co-orbital Lindblad resonance, and as the arguments of § 3 demonstrate, it leads to eccentricity damping. However, preliminary investigation shows that it is of little importance.

Our mechanism of eccentricity growth can be tested by numerical simulations. Recently, Papaloizou et al. (2001) observed eccentricity growth for planets larger than about 10–20 M_J in an $\alpha = 4.5 \times 10^{-3}$ disk. With these parameters the gap extends past the 2 : 1 resonance, rendering all first-order corotation resonances impotent. Similar behavior was observed earlier by Artymowicz et al. (1991) for binary stars surrounded by a disk. Both papers appear to support our claim that the apsidal resonance does not damp eccentricity as fast as external Lindblad resonances excite it. In apparent contradiction to our conclusions, Papaloizou et al. (2001) did not find eccentricity growth for Jovian mass planets. Several explanations come to mind. Limitations of our analysis may have led us to predict eccentricity growth where it does not occur. Alternatively, their simulations may lack sufficient resolution to capture the partial saturation of corotation resonances. Numerical simulation of orbital evolution of planets embedded in disk should be analyzed to identify the source and sinks of energy and angular momentum. Only in this way can issues involving the saturation of corotation resonances and damping by apsidal waves be settled.

This research was supported in part by NSF grant AST 00-98301 and NASA grant NAG5-12037 awarded to P. G. and a Sherman Fairchild Senior Fellowship held by R. S. We thank Geoff Bryden and Jeremy Goodman for several illuminating conversations. We are particularly indebted to Gordon Ogilvie and Steven Lubow for alerting us to their preprint on corotation saturation in gas disks. This saved us from publishing an erroneous result and led to a substantial improvement of § 6.

REFERENCES

Artymowicz, P. 1993a, ApJ, 419, 166
———. 1993b, ApJ, 419, 155
Artymowicz, P., Clarke, C. J., Lubow, S. H., & Pringle, J. E. 1991, ApJ, 370, L35
Borderies, N., Goldreich, P., & Tremaine, S. 1982a, Nature, 299, 209
———. 1982b, Science, 299, 209
Bryden, G., Różyczka, M., Lin, D. N. C., & Bodenheimer, P. 2000, ApJ, 540, 1091
Chiang, E. I., Fischer, D., & Thommes, E. 2002, ApJ, 564, L105
Ford, E. B., Havlickova, M., & Rasio, F. A. 2001, Icarus, 150, 303
Goldreich, P., & Tremaine, S. 1978, Icarus, 34, 240
———. 1979, ApJ, 233, 857
———. 1980, ApJ, 241, 425
———. 1981, ApJ, 243, 1062
Goodman, J., & Rafikov, R. R. 2001, ApJ, 552, 793
Kim, S. S., & Lee, H. M. 1999, A&A, 347, 123
Lee, E., & Goodman, J. 1999, MNRAS, 308, 984
Lin, D. N. C., & Ida, S. 1997, ApJ, 477, 781
Lynden-Bell, D., & Kalnajs, A. J. 1972, MNRAS, 157, 1
Ogilvie, G. I. 2001, MNRAS, 325, 231
Ogilvie, G. I., & Lubow, S. H. 2002, ApJ, submitted (astro-ph/0208363)
Papaloizou, J. C. B. 2002, A&A, 388, 615
Papaloizou, J. C. B., Nelson, R. P., & Masset, F. 2001, A&A, 366, 263
Rasio, F. A., & Ford, E. B. 1996, Science, 274, 954
Tremaine, S. 2001, AJ, 121, 1776
Ward, W. R. 1986, Icarus, 67, 164
———. 1988, Icarus, 73, 330
Ward, W. R., & Hahn, J. M. 1998, AJ, 116, 489
———. 2000, in Protostars and Planets IV, ed. V. Mannings, A. P. Boss, & S. S. Russell (Tucson: Univ. Arizona Press), 1135
Weidenschilling, S. J., & Marzari, F. 1996, Nature, 384, 619